Molecular Cell, Volume *44*

Supplemental Information

Mechanism of USP7/HAUSP Activation by Its C-Terminal Ubiquitin-like Domain and Allosteric Regulation by GMP-Synthetase

Alex C. Faesen, Annette M.G. Dirac, Anitha Shanmugham, Huib Ovaa, Anastassis Perrakis, and Titia K. Sixma

Inventory of Supplemental Information

Faesen et al. Supplementary Figure S1

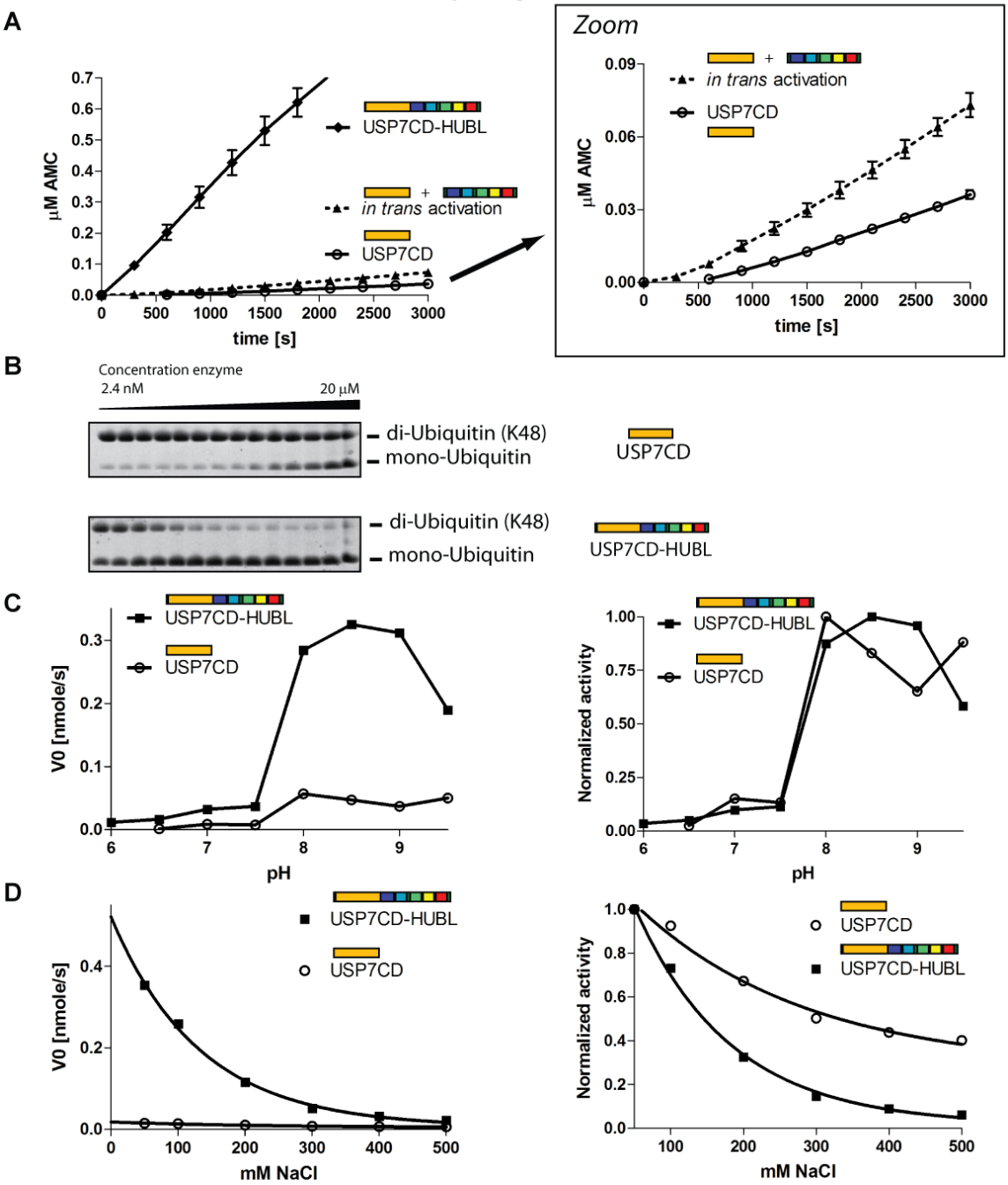

Figure S1 related to Figure 1. A. USP7CD can be activated both *in trans* and *in cis* by the HUBL domain. Using 1 µM UbiAMC and 1 nM USP7, the activity decreases strongly in the absence of the HUBL domain. This loss can be partially recovered by adding 10 µM HUBL to USP7CD. **B.** USP7CD concentrations need to be 1000-fold increased to achieve the same catalytic turn-over as USP7CD-HUBL. **C.** The pH profile was determined of the USP7 activity was monitored using 1 µM UbiAMC. Both USP7CD and USP7CD-HUBL show a similar pH profile, but it is more pronounced with USP7CD-HUBL due to the higher catalytic rate. **D.** The activity of both USP7CD and USP7CD-HUBL decrease upon increasing NaCl concentration, with a limited strengthening effect of the HUBL domain.

Faesen et al. Supplementary Figure S2

A

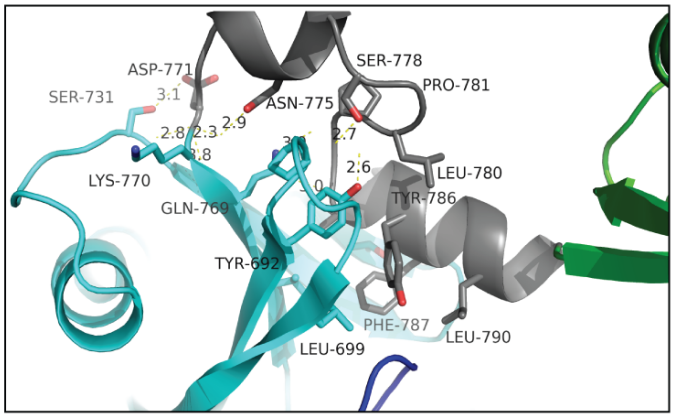

Interface Area [Å²]	742.3
ΔiG [kcal/mole]	-7.1
# H-bonds	10
# Salt bridges	2

B

Cα rmsd [Å] ←

HUBL	1	2	3	4	5	Ubiquitin
1		2.5	2.1	2.9	2.8	2.0
2	9.1		2.5	2.6	2.7	1.9
3	10.6	9.1		2.9	2.6	2.0
4	9.1	15.2	6.1		2.9	2.5
5	7.6	3.0	12.1	7.6		2.5
Ubiquitin	19.7	12.1	9.1	6.1	15.2	

→ Sequence identity [%]

C

D

	1-2	2-3	3-4	4-5
Interface Area [Å²]	1199.4	171.1	0	738.7
ΔiG [kcal/mole]	-10.5	0.440		-8.3
# H-bonds	19	1	0	7
# Salt bridges	6	0	0	4

E

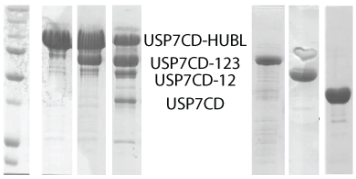

Figure S2 related to Figure 2. A. The second helix in the linker region between HUBL-2 and -3 interacts with HUBL-2. Left: Cartoon representation, colours as in Figure 2, Right: Interface parameters, calculated with SSM (Krissinel and Henrick, 2004). **B.** Despite the homologous fold, which is quantified by the low Cα rmsd, the primary sequence identity between the Ubl's and with ubiquitin is low. Numbers based on the alignment in C. **C.** Structure based sequence alignment using SSM shows that the Ubl's share the β-grasp fold with ubiquitin. **D.** Interface analysis by PISA (Krissinel and Henrick, 2004) revealed extensive interactions between HUBL-1 and -2 and HUBL-4 and -5. **E.** The Ubl domains within HUBL group in a 2-1-2 configuration in solution. USP7CD-HUBL degrades during purification to stable intermediates with masses corresponding to USP7CD-123, USP7CD-12 and USP7CD.

Faesen et al. Supplementary Figure S3

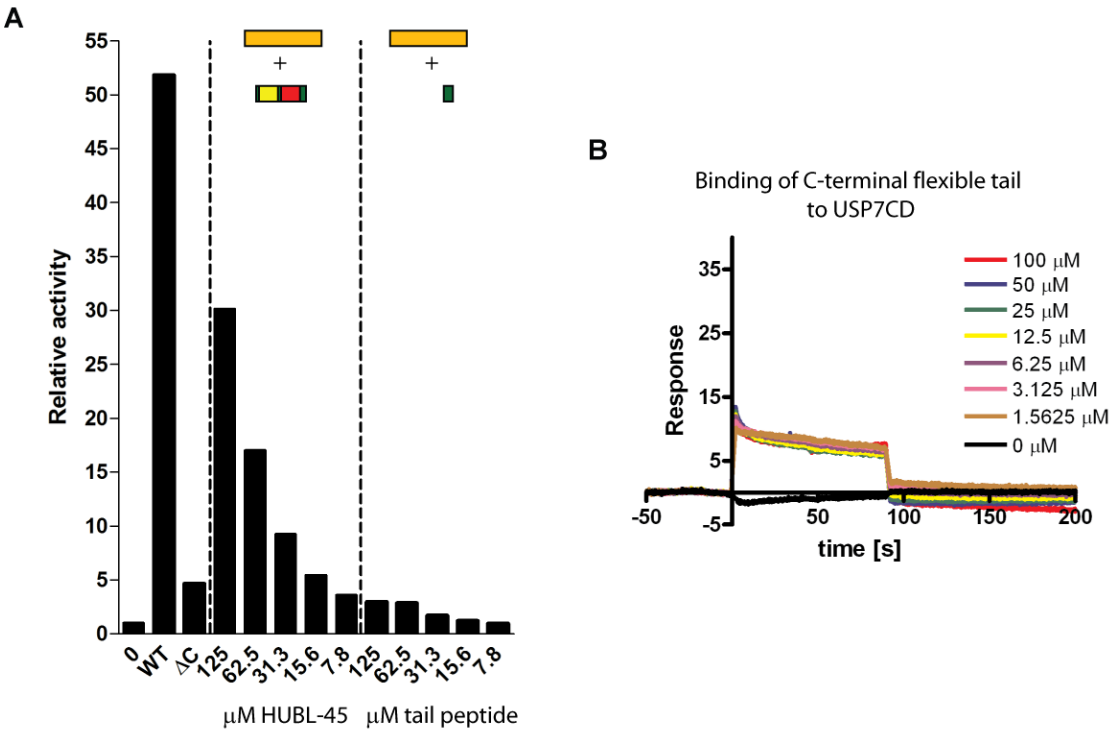

Figure S3 related to Figure 4. The C-terminal peptide is essential, but not sufficient, for activation. A. Activity on Ub-AMC shows that upon removal of the C-terminal 19 residues in the flexible peptide loop (ΔC), the activation by the HUBL domain is greatly reduced. However, this peptide is not sufficient to achieve *in trans* activation, to similar levels as complete HUBL-45. **B.** Using SPR, no binding between USP7CD and the C-terminal peptide is observed. The responses are due to aspecific binding to the SPR chip and show no concentration dependence.

Faesen et al. Supplementary Figure S4

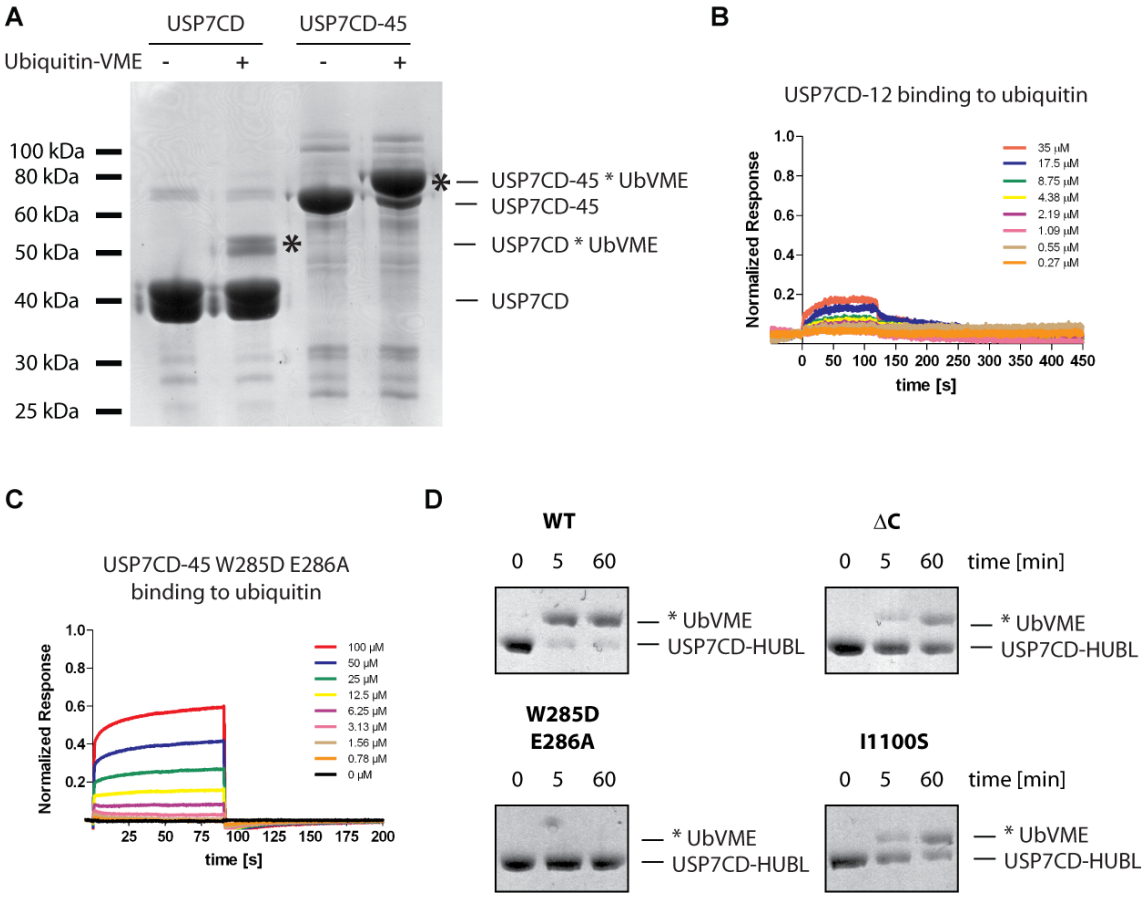

Figure S4 related to Figure 5. Ubiquitin affinity is increased by the HUBL domain. A. When incubated with 20 µM suicide substrate ubiquitin-VME (Borodovsky et al., 2002), only USP7CD-45 and not USP7CD was robustly able to form covalent complexes with ubiquitin as shown in this Coomassie stained SDS PAGE gel. Asterisk shows the USP7-ubiquitin complex. **B.** Using SPR binding experiments, very weak binding to ubiquitin was observed for USP7CD-12. GST-ubiquitin was immobilized to the CM5 sensor chip. **C.** Mutations in the 'switching loop' lower affinity for ubiquitin. SPR Sensorgram of the ubiquitin binding of USP7CD-45 W285D E286A (Kd = 65µM). **D.** When incubated with 5 µM suicide substrate ubiquitin-VME, only WT USP7 and not the mutants was robustly able to form covalent complexes with ubiquitin as shown in Coomassie stained SDS PAGE gel. Asterisk shows the USP7-ubiquitin complex.

Faesen et al. Supplementary Figure S5A

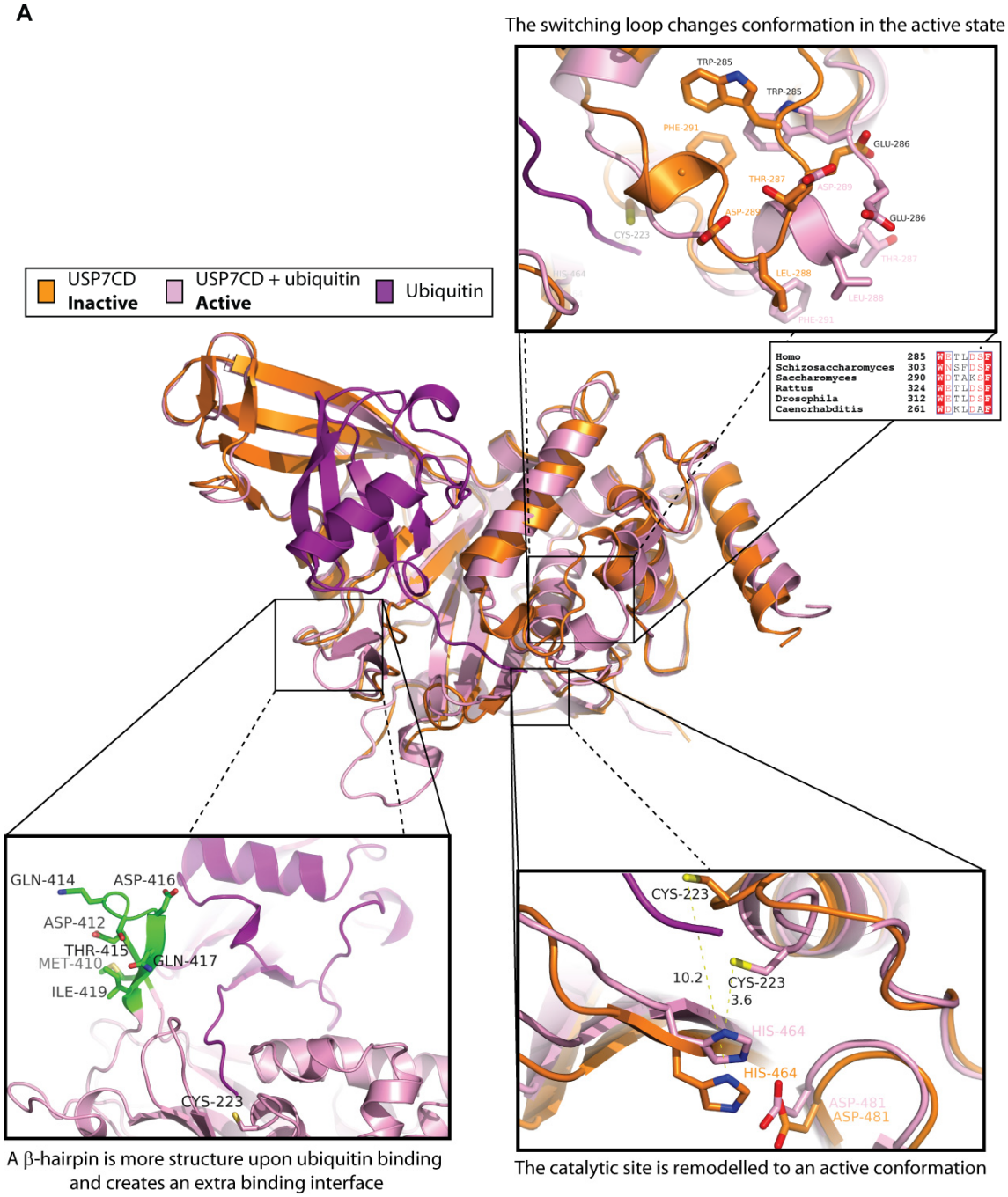

Figure S5 related to Figure 6. Crystal structure of USP7CD shows conformational changes upon remodelling of the active site and ubiquitin binding. A. Comparison of the apo structure of USP7CD (1NB8), with the ubiquitin complex of USP7CD (1NBF) (Hu et al 2006) show movement of a β-hairpin (bottom left), organization of the active site (bottom right) and remodelling of a 'switching loop' (top right), for which the sequence conservation is indicated.

Faesen et al. Supplementary Figure S5B

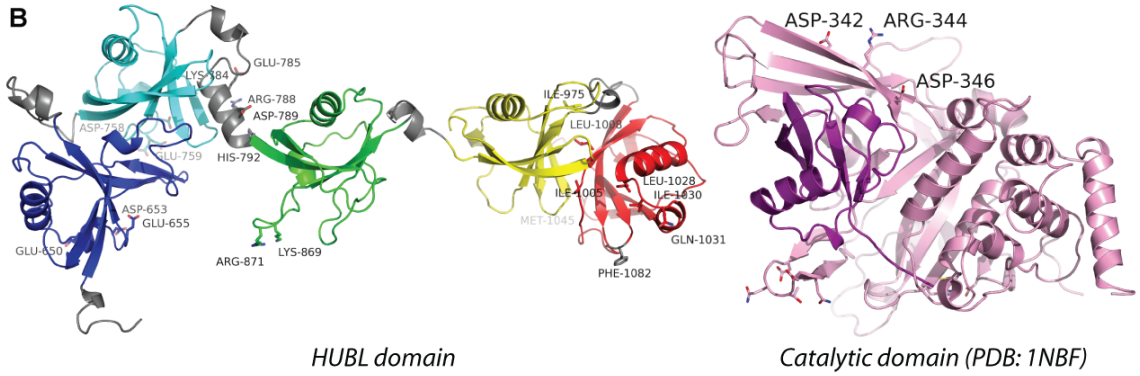

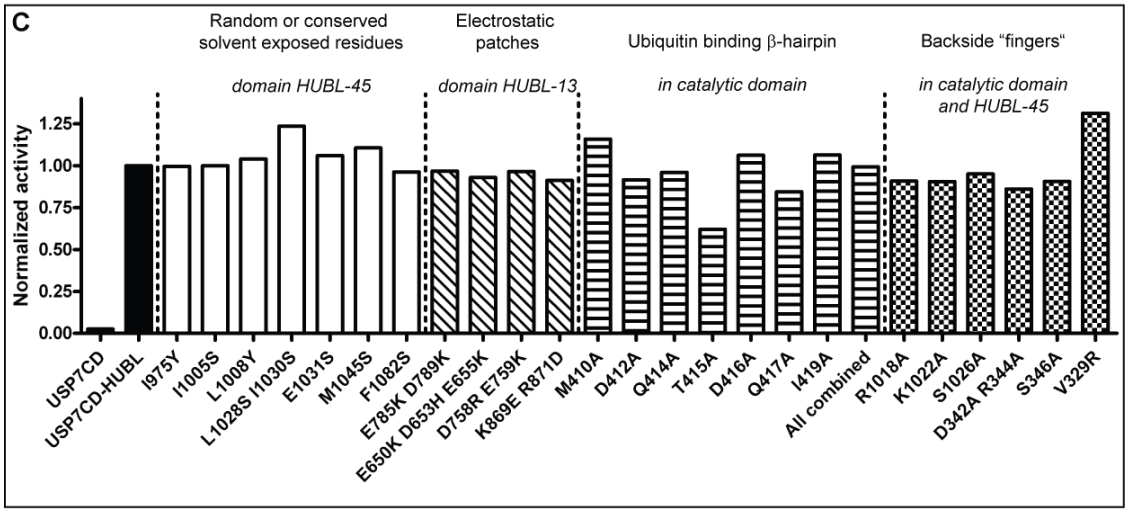

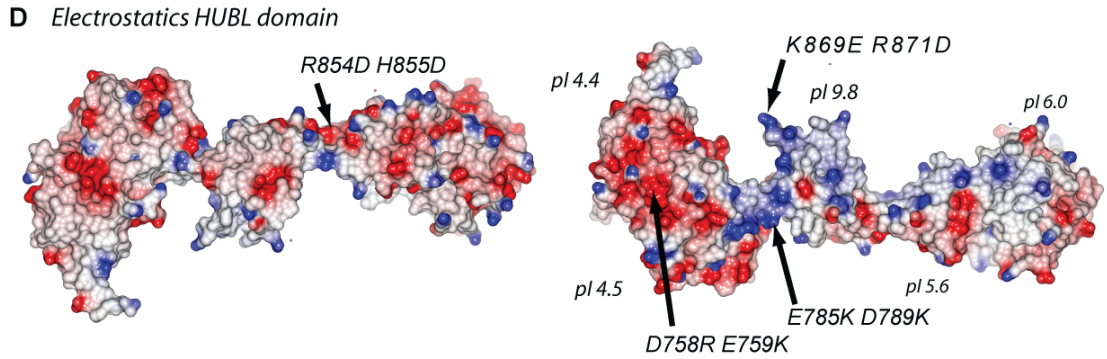

B-D. Overview mutations. A priori, three possible activation mechanisms could be envisaged, i) the stabilization of a β-hairpin in the catalytic domain (residues 410 to 420), which is more structured when co-crystallized with ubiquitin, making an extra interface with ubiquitin, ii) restricting the movement of the "finger region", as is achieved in other DUBs by the insertion of an extra helix that stabilizes the fingers domain, or iii) near the active site there is dynamic switching of a loop that dependents on ubiquitin binding. However, since mutations within the ubiquitin binding β-hairpin or the backside of the "finger region" did not have an effect on activation by the HUBL domain, we excluded the first two possibilities. Domains are depicted in cartoon respresentation and the mutants are show in sticks. The activity is normalized to full length USP7. The electrostatic potential is calculated using CCP4MG (Potterton et al., 2004).

Faesen et al. Supplementary Figure S6

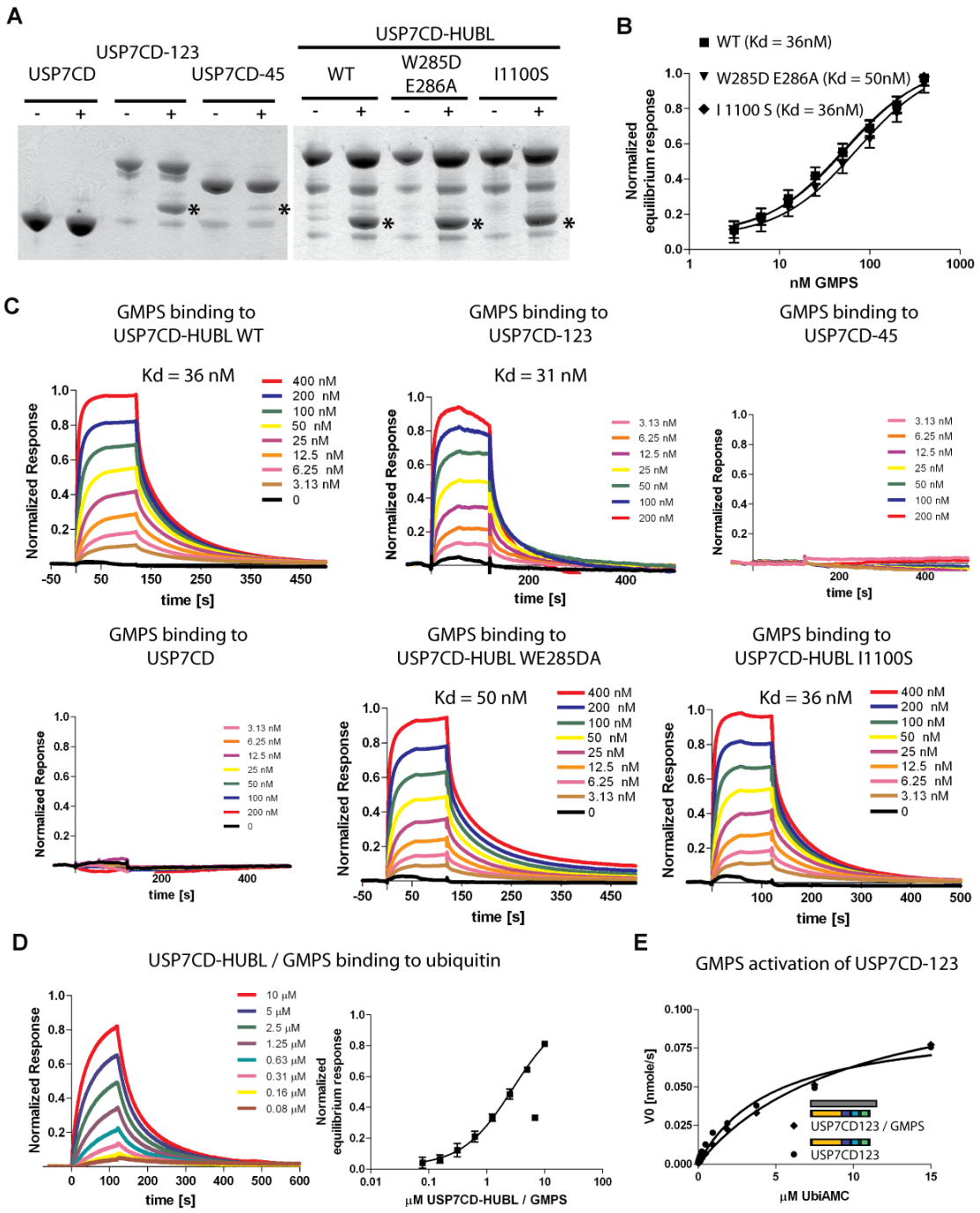

Figure S6 related to Figure 7. GMPS activation and binding. A. GMPS can only robustly be pulled down by GST-tagged USP7 constructs containing HUBL-123. **B and C.** Equilibrium responses (D) and sensorgrams (E) of GMPS binding to USP7 constructs and mutants. Using SPR a Kd of 30-40 nM was determined between USP7CD-HUBL and GMPS. The mutants WE285DA and I1100S, and USP7CD-13 behaved similar as wild-type in GMPS binding. No binding was observed for USP7CD and USP7CD-45. **D.** SPR sensorgram of USP7CD-HUBL/GMPS binding ubiquitin (Kd = 2.5µM). **E.** USP7CD-123 can not be hyper-activated by GMPS in the Ub-AMC assay.

Faesen et al. Supplementary Table S1

	k_{cat} [s^{-1}]	K_m [μM]	k_{cat}/K_m [M^{-1} s^{-1}]	Ub K_d [μM]
USP7FL	1.42 ± 0.02	2.89 ± 0.10	4.92 *10^5	n.d.
USP7CD-HUBL	1.35 ± 0.06	3.62 ± 0.42	3.72 *10^5	1.5 ± 0.5
USP7CD	0.06 ± 0.02	15.13 ± 1.09	0.04 *10^5	>>35
USP7CD-45	1.32 ± 0.03	2.89 ± 0.20	4.57 *10^5	4.0 ± 0.6
USP7CD + HUBL	0.29 ± 0.03	14.67 ± 1.98	0.20 *10^5	12.9 ± 1.4
USP7CD-HUBL WE285DA	0.31 ± 0.05	9.80 ± 0.59	0.32 *10^5	65.0 ± 5.3
USP7CD-HUBL I1100S	0.07 ± 0.02	10.51 ± 0.58	0.07 *10^5	n.d.
USP7CD-HUBL / GMPS	7.69 ± 0.23	8.95 ± 0.53	8.60 *10^5	2.5 ± 0.2
USP7CD-HUBL WE285DA / GMPS	0.32 ± 0.05	10.78 ± 0.59	0.30 *10^5	n.d.
USP7CD-HUBL I1100S / GMPS	0.07 ± 0.001	13.05 ± 0.13	0.05 *10^5	n.d.

Table S1.
Summary of the kinetic data determined in Ub-AMC assays and ubiquitin binding, determined using SPR

Supplemental Experimental Procedures

General plasmids, proteins, antibodies

Plasmids for human MDM2, MDMX were a gift from Martin Scheffner, plasmids encoding ubiquitin variants for chain formation were a gift from Shaari Rahzi. Purified hyperstable p53 (Khoo et al., 2009) was a gift from Caroline Blair and Alan Fersht, UBA1, UBCH5c, ubiquitin were purified as described (Buchwald et al., 2006; Pickart and Raasi, 2005); human MDM2/MDMX was purified using Martin Scheffner's protocol (Linares et al., 2003), di-ubiquitin with a K48 linkage was produced as previously described (Pickart and Raasi, 2005).

Generation of plasmids, bacmids and baculoviruses

Codon optimized full length USP7 and GMPS cDNA was obtained from DomainEx (Cambridge, UK). Both were amplified by PCR and subcloned (SpeI/NotI) into a pFastBac vector (Invitrogen) containing an N-terminal GST tag (BamHI/SpeI) and Prescission Protease cleavage site. Bacmids were prepared following the manufacturer's guidelines. Virus was produced using the low-MOI infection protocol (Fitzgerald et al., 2006). DNAs coding for the truncation and deletion constructs of USP7 were amplified with 5'-BamHI and 3'-NotI overhangs and subcloned into the pGEX-6P-1 vector (GE Healthcare) or by introducing stop codons using the QuickChange mutagenesis kit from Stratagene (La Jolla, CA, USA). All constructs were checked by sequencing. USP7CD-45 was produced by amplifying the catalytic domain (residues 208 to 564) with 5'-BamHI and 3'-XhoI overhangs and HUBL-45 (residues 890 to 1102) 5'-XhoI and 3'-NotI overhangs and both fragment subsequently subcloned into the pGEX-6P-1 vector (GE Healthcare). This resulted in the addition of two extra residues (Leu-Glu) between the catalytic domain and HUBL-45. Mutants were created with the QuickChange mutagenesis kit (Stratagene).

Protein expression and purification

Full length USP7 and GMPS were produced using *Sf9* and *Sf21* insect cell expression. Infection was done using a low-MOI infection protocol (Fitzgerald et al., 2006). The cells were harvested 72 hours after a baculovirus induced growth arrest was observed. All USP7 truncation constructs, USP7 mutants and GST-ubiquitin were expressed in *E.coli* BL21(DE3) T1-R cells using auto-induction medium (Studier, 2005) overnight at 15°C. Selenomethionine HUBL was produced for crystallization and was expressed in *E.coli* B834(DE3) T1-R cells using SelenoMet Medium Base (Athena Enzyme Systems). All proteins were purified using GST sepharose (GE Healthcare) in 50 mM Hepes (pH 7.5), 250 mM NaCl, 0.1 mM PMSF, 1 mM EDTA and 1 mM DTT followed by elution in 50 mM reduced glutathione and overnight cleavage by Prescission Protease (GE Healthcare). Size exclusion chromatography was performed using a Superdex 200 or 75 column (GE Healthcare), equilibrated against buffer containing 10 mM Hepes [pH 7.5], 100 mM NaCl and 1 mM DTT. All proteins eluted as monomers from the gel filtration. When necessary the cleaved GST-tag was removed by attaching a GST FF column (GE Healthcare) to the end of the gel filtration column. USP7/GMPS complexes were purified using co-lysis, or mixing of the individual proteins before the last gel-filtration. Protein was concentrated to ~10 mg/ml and stored at -80°C.

In vitro p53 de-ubiquitination assay

Purified hyperstable p53 (Khoo et al., 2009) was ubiquitinated using 0.5 μM Uba1, 3 μM UbcH5c, human MDM2/MDMX, 250nM p53, 2 μM ubiquitin and 10mM ATP in 25 mM Tris (pH 8.0), 150 mM NaCl, 10 mM $MgCl_2$, 2 μM $ZnCl_2$, 5 μM β-mercapto-ethanol and 1 mM DTT for 1 hour at 37 degrees. The reaction was stopped by adding 11 mM EDTA and incubated with varying concentrations of USP7 for 1 hour at 37 degrees. Western blot was

performed using mouse 1:1000 p53 antibody (PAB240 Santa Cruz) and the Pierce Fast Western Blot Kit.

Cell cultures, transient transfections

U2OS cells were cultured in Dulbecco's modified eagle medium (DMEM), supplemented with 10% foetal calf serum. Transfections were done with the calcium phosphate method. Cells were transfected with 10 µg GFP-USP7 construct and 0.5 µg pBabePuro per 10 cm dish. 48 hours after transfection, cells were selected with puromycin. Puromycin selected cells were lysed in RIPA buffer supplemented with "complete" protease inhibitors (Roche). Western blots were performed using whole cell extracts, separated on 8% SDS-PAGE gels and transferred to polyvinylidine difluoride membranes (Millipore). Western blots were probed with the indicated antibodies. Antibodies used were anti-GFP (FL), p53 (DO-1), and MDM2 (SMP-14), Hsp90 α/β (H-114), all from Santa Cruz.

Di-ubiquitin assay

Di-ubiquitin hydrolysis reactions were performed at 37°C in 50 mM Hepes buffer (pH 7.5), 100mM NaCl, 1 mM EDTA, 5 mM DTT and 0.05% (w⁄v) Tween-20 with either constant enzyme concentration (50nM) or constant substrate concentration (10 µM) with two-fold serial dilutions of the USP7 construct (starting from 20 µM). Reactions were stopped by addition of SDS loading buffer.

Ubiquitin-AMC assay

Activity towards Ub-AMC (Sigma) was assayed at 25°C in 50 mM Hepes buffer (pH 7.5), 100mM NaCl, 1 mM EDTA, 5 mM DTT and 0.05% (w⁄v) Tween-20. Assays were performed in "Non binding surface flat bottom low flange" black 384-well plates (Corning) in a 30 µl reaction volume. Fluorescence was measured in intervals of 5 min using a Fluostar Optima plate reader (BMG Labtechnologies) at excitation and emission wavelengths of 355 nm and 460 nm, respectively. All assays were performed in triplicate.

Kinetic analysis with Ubiquitin-AMC assay

To determine the assay linearity range, serial dilutions (from 200 nM) of each USP7 construct were used to completely hydrolyze 1 µM of Ub-AMC. For Michaelis-Menten analysis, constant enzyme concentrations (1nM for full length USP7, USP7CD-HUBL and USP7CD45; 10 nM for USP7CD) were used to hydrolyze varying substrate concentrations (from 15 µM in two-fold dilutions). In order to calculate the kinetic parameters for the hydrolysis of Ub-AMC, curves obtained by plotting the measured enzyme initial rates (v) versus the corresponding substrate concentrations ([S]). These were subjected to nonlinear regression fit using the Michaelis–Menten equation $V = (V_{max} \cdot [S]) / ([S] + K_m)$ (eqn 1), where Vmax is the maximal velocity at saturating substrate concentrations and Km the Michaelis constant. The kcat value was derived from the equation $k_{cat} = V_{max} / [E_o]$ (eqn 2) where [Eo] is the total enzyme concentration. Experimental data was processed using Prism 4.03 (GraphPad Software, Inc.).

Crystal structure determination

For data collection statistics, see Table S1. HUBL (residues 560 to 1102) was crystallized at 4°C in sitting drops against 10% (w/v) PEG4000, 200 mM sodium chloride, and 100 mM MES at pH 6.0 and cryoprotected in mother liquor supplemented with 20% (w/v) glycerol. A single-wavelength anomalous diffraction (SAD) experiment at the selenium anomalous peak wavelength, was performed at the PX beamline at the Swiss Light Source (SLS), while a native data set was collected at the ESRF microfocus beamline ID23-2. Both data sets were

collected from a single crystal at 100K. Diffraction images were integrated with iMOSFLM (Leslie, 2006) and scaled with SCALA (Evans, 2006), to 3Å for the selenomethionine crystal and 2.7Å for the native crystal. Structure solution was carried out using SHARP/autoSHARP (Vonrhein et al., 2007), and resulted to a phase probability distribution with an overall figure of merit of 0.47 before solvent flattening. ARP/wARP (Langer et al., 2008) was used to built an initial incomplete model (375 out of 547 residues) which was used as a template to build a model manually in Coot (Emsley and Cowtan, 2004). This refined in iterative cycles with PHENIX (Adams et al., 2010) and Buster (Blanc et al., 2004). For crystallographic parameters, see Table S1. For residues 1084-1102, no electron density has been observed. Structure figures were generated using PyMOL (http://www.pymol.org). Pictures of the electrostatic potential mapped on the protein surface were generated using CCP4MG (Potterton et al., 2004). Further structural analysis was performed with Espript (Gouet et al., 1999), PISA (Krissinel and Henrick, 2007), DSSP (Kabsch and Sander, 1983) and SSM (Krissinel and Henrick, 2004).

SAXS analysis

Samples for the SAXS experiments were prepared immediately after gel filtration in buffer containing 10 mM Hepes [pH 7.5], 100 mM NaCl and 1 mM DTT with an additional 5% (v/v) glycerol as a radiation scavenger. Samples were taken during concentration and the flow-through was collected and used for the blank measurements. Typically five concentrations were measured, ranging from 0.5 to 10 mg/ml. Data were collected at the ESRF beamline ID14-3. Data were processed, analysed and modelled using programs from the ATSAS software package (Svergun et al., 2001). For the HUBL domain aggregation was observed and only the lowest concentration was used. The interatomic distance distribution probability function *P(r)* was calculated using Gnom. Rigid body modeling was performed using SASREF, using individual Ubl domains and/or the di-Ubl units. Distance constraints to define covalent links, or linkers when the connecting loops were removed, yielded similar results as using no distance restraints. Where possible, multiple merged scattering curves were used when the constructs overlapped. The *ab initio* models were calculated by DAMMIF and averaged over ten models using DAMAVER.

Surface Plasmon Resonance (SPR)

SPR was performed at 25°C on a Biacore T100. A CM5 sensor chip was prepared with monoclonal GST antibody via amino coupling (~20000 response units). This chip was used to load roughly 50 response units of GST-ubiquitin or 400 response units of GST-USP7CD. Biotinylated peptides were coupled to a SA chip (200 RU's). Concentration series of the USP7 constructs in running buffer (10 mM HEPES [pH 7.5], 100mM NaCl, 5 mM DTT, and 0.05% Tween-20) were tested at 30 µl/min. Saturation binding values were plotted against concentration (GST as reference) and fit to a steady-state affinity model for calculation of apparent dissociation (Kd) and association (Ka) constants (Prism 4.03, GraphPad Software, Inc.). All experiments have been repeated at least three times.

Supplemental References

1. Borodovsky, A., Ovaa, H., Kolli, N., Gan-Erdene, T., Wilkinson, K.D., Ploegh, H.L., and Kessler, B.M. (2002). Chemistry-based functional proteomics reveals novel members of the deubiquitinating enzyme family. Chemistry & biology *9*, 1149-1159.
2. Buchwald, G., van der Stoop, P., Weichenrieder, O., Perrakis, A., van Lohuizen, M., and Sixma, T.K. (2006). Structure and E3-ligase activity of the Ring-Ring complex of polycomb proteins Bmi1 and Ring1b. The EMBO journal *25*, 2465-2474.
3. Fitzgerald, D.J., Berger, P., Schaffitzel, C., Yamada, K., Richmond, T.J., and Berger, I. (2006). Protein complex expression by using multigene baculoviral vectors. Nature methods *3*, 1021-1032.
4. Khoo, K.H., Joerger, A.C., Freund, S.M., and Fersht, A.R. (2009). Stabilising the DNA-binding domain of p53 by rational design of its hydrophobic core. Protein Eng Des Sel *22*, 421-430.
5. Krissinel, E., and Henrick, K. (2004). Secondary-structure matching (SSM), a new tool for fast protein structure alignment in three dimensions. Acta crystallographica *60*, 2256-2268.
6. Linares, L.K., Hengstermann, A., Ciechanover, A., Muller, S., and Scheffner, M. (2003). HdmX stimulates Hdm2-mediated ubiquitination and degradation of p53. Proceedings of the National Academy of Sciences of the United States of America *100*, 12009-12014.
7. Pickart, C.M., and Raasi, S. (2005). Controlled synthesis of polyubiquitin chains. Methods in enzymology *399*, 21-36.
8. Potterton, L., McNicholas, S., Krissinel, E., Gruber, J., Cowtan, K., Emsley, P., Murshudov, G.N., Cohen, S., Perrakis, A., and Noble, M. (2004). Developments in the CCP4 molecular-graphics project. Acta crystallographica *60*, 2288-2294.
9. Studier, F.W. (2005). Protein production by auto-induction in high density shaking cultures. Protein expression and purification *41*, 207-234.